Journal of Materials Chemistry

Cite this: J. Mater. Chem., 2011, 21, 3796

www.rsc.org/materials

PAPER

Intermolecular energy transfer and photostability of luminescence-tuneable multicolour PMMA films doped with lanthanide–β-diketonate complexes†

Jiang Kai,[ab] Maria C. F. C. Felinto,[b] Luiz A. O. Nunes,[c] Oscar L. Malta[d] and Hermi F. Brito*[a]

Received 14th October 2010, Accepted 21st December 2010
DOI: 10.1039/c0jm03474f

It is reported in this work the preparation, characterisation and photoluminescence study of poly(methylmethacrylate) (PMMA) thin films co-doped with $[Eu(tta)_3(H_2O)_2]$ and $[Tb(acac)_3(H_2O)_3]$ complexes. Both the composition and excitation wavelength may be tailored to fine-tune the emission properties of these Ln^{3+}–β-diketonate doped polymer films, exhibiting green and red primary colours, as well as intermediate colours. In addition to the ligand–Ln^{3+} intramolecular energy transfer, it is observed an unprecedented intermolecular energy transfer process from the $^5D_4$ emitting level of the Tb^{3+} ion to the excited triplet state T_1 of the tta ligand coordinated to the Eu^{3+} ion. The PMMA polymer matrix acts as a co-sensitizer and enhances the overall luminescence intensity of the polymer films. Furthermore, it provides considerable UV protection for the luminescent species and improves the photostability of the doped system.

1. Introduction

Interest in luminescent materials containing trivalent lanthanide ions (Ln^{3+}) as emitting centres has grown significantly in recent years.[1] The electronic energy levels are little affected by their chemical environments due to the effective shielding of the 4f electrons by the filled 5s and 5p external sub-shells.[2] Consequently, the spectra of the 4f–4f intraconfigurational transitions of the Ln^{3+} ions retain more or less their atomic character, making Ln^{3+}-based luminescent materials suitable for advanced photonic applications in optoelectronic devices,[3] biological fluorescence labelling,[4] white light-emitting devices,[5] multicolour pigments[6] and colour-tuneable phosphors.[7]

In the design of highly luminescent Ln^{3+}-complexes, it is essential to optimize the ligand–Ln^{3+} energy transfer process in order to maximize the emission originated from 4f–4f intraconfigurational transitions.[8] A simplified mechanism for Ln^{3+}-complex luminescence is described as follows: (i) strong absorption from the ground singlet state (S_0) to the excited singlet state (S_1) of the ligand; (ii) state S_1 decays non-radiatively to the triplet state (T_1) *via* intersystem crossing and (iii) non-radiative energy transfer pathway from the T_1 state of the ligand to excited states of the Ln^{3+} ion. In some cases direct energy transfer from the S_1 singlet state to excited Ln^{3+} levels is also of importance.[2]

However, the Ln^{3+}-complexes generally present low thermal stability, limited photostability and poor mechanical properties. Another parallel challenge is that most of these compounds are usually achieved as hydrates, consequently the luminescence intensity is suppressed due to the activation of non-radiative channels.[1,2] In order to overcome simultaneously these deficiencies and improve the characteristics of light emission (*e.g.* quantum yield, lifetimes), Ln^{3+}-complexes have been incorporated into organic polymers, liquid crystals and sol–gel derived organic–inorganic hybrids.[1] Polymers offer several advantages for the development of materials, such as: flexibility, versatility, optical quality and moderate processing conditions. By incorporating luminescent Ln^{3+}-complexes within the polymer matrix, the resulting product represents not only the sum of individual contributions of both organic and inorganic phases, but also novel properties for a new class of materials.[9]

The poly(methylmethacrylate) polymer (PMMA) exhibits excellent mechanical and optical properties that favour its application as the basis for optical devices.[10] Furthermore, PMMA contains carbonyl groups along with its carbon-chain that can interact with Ln^{3+} ions and substitute ligand water molecules. Hence, improvement in the overall physical and chemical properties and enhancement of the characteristics of emission quantum yield and lifetimes can be expected with polymer films based on PMMA doped with Ln^{3+}–β-diketonate complexes.

[a]*Departamento de Química Fundamental, Instituto de Química, Universidade de São Paulo, 748 Av. Prof. Lineu Prestes, 05508-000 São Paulo, SP, Brazil. E-mail: hefbrito@iq.usp.br; Fax: +55 11 38155579; Tel: +55 11 30913708*
[b]*Centro de Química e Meio Ambiente, Instituto de Pesquisas Energéticas e Nucleares, 2242 Av. Prof. Lineu Prestes, 05508-000 São Paulo, SP, Brazil*
[c]*Instituto de Física de São Carlos, Universidade de São Paulo, 400 Av. Trabalhador São-Carlense, 13566-590 São Carlos, SP, Brazil*
[d]*Departamento de Química Fundamental—CCEN, Universidade Federal de Pernambuco, Cidade Universitária, 50740-540 Recife, PE, Brazil*

† Electronic supplementary information (ESI) available: IR, additional TGA and emission spectra of PMMA films doped with $[Eu(tta)_3(H_2O)_2]$. See DOI: 10.1039/c0jm03474f

In the present work, diaquatris(thenoyltrifluoroacetonate)-europium(III), $[Eu(tta)_3(H_2O)_2]$, and triaquatris(acetylacetonate)-terbium(III), $[Tb(acac)_3(H_2O)_3]$, complexes were utilized as precursors and incorporated into the PMMA polymer in order to obtain multicolour light-emitting devices due to their strong luminescence and relatively simple and inexpensive preparations. The triplet state T of the acac ligand is located around 26 000 cm^{-1} and in resonance with the excited $^5D_4$ level (20 400 cm^{-1}) of the Tb^{3+} ion, resulting in a highly efficient sensitisation pathway in the $[Tb(acac)_3(H_2O)_3]$ complex.[11] A similar behaviour can be observed for the $[Eu(tta)_3(H_2O)_2]$ complex whereas the T state of the tta ligand (20500 cm^{-1}) is also in resonance with the excited $^5D_0$ and $^5D_1$ levels of the Eu^{3+} ion around 17 300 and 19 000 cm^{-1}, respectively.[2] The most relevant aspect of this work is that the colour tuning between the green and red may be obtained either by varying the excitation wavelength or the relative concentrations of the complexes in the polymer matrix.

2. Results and discussion

2.1. Characterisation

In general, the powder X-ray diffraction patterns in amorphous systems present broadened peaks. However, in the present case,it is observed an increasing crystallinity for the PMMA:Eu-$(tta)_3$:$Tb(acac)_3$ films with doping concentration from 1 to 15% in mass (Fig. 1), induced by the progressive incorporation of the Ln^{3+} complexes into the polymer matrix. These results confirmed the successful synthesis and incorporation of the complexes: $[Ln(tta)_3(H_2O)_2]$ (Ln = Eu^{3+} and Gd^{3+}) and $[Tb(acac)_3(H_2O)_3]$ into the PMMA polymer matrix, also corroborating with infrared absorption spectroscopy (ESI†, Fig. S1 and S2).

The thermogravimetric analysis (TGA) of the co-doped PMMA:$Ln(tta)_3$:$Tb(acac)_3$ films under dynamic N_2 atmosphere showed no significant change of the T_{onset} (~300 °C) compared with the undoped polymer. Furthermore, it can be observed in Table S1† that the major weight-loss events occur at the same temperature interval (300–425 °C). These results indicate that the thermal decomposition behaviour of the polymer films was little affected by the doping process with the complex precursors (Fig. 2). On the other hand, the Ln^{3+}–β-diketonate complexes generally begin thermal decomposition at around 200 °C,[12] showing that the incorporation of these complexes into the PMMA matrix increases the overall thermal stability.

Another important observation from the TGA data is that no weight-loss event was observed within 150–220 °C for all PMMA polymer films doped with the Ln^{3+}-complex precursors (Fig. 2, S3†). This reveals that after the doping process the water molecules coordinated to the Ln^{3+} ion of the hydrated complexes are replaced by the interaction between the Ln^{3+} ions and the oxygen atoms of the carbonyl group in the PMMA backbone. This result also corroborates with the IR data, as the broad band centred around 3400 cm^{-1} assigned to the characteristic O–H oscillators of the water molecules in the first coordination sphere found for both $[Eu(tta)_3(H_2O)_2]$ and $[Tb(acac)_3(H_2O)_3]$ complexes is absent in all IR spectra of the Ln^{3+} doped PMMA films (Fig. S1 and S2†).

2.2. Photoluminescence behaviour

Based on the emission spectra of the PMMA:x%$Eu(tta)_3$ films (x = 1, 5, 10 and 15) and $[Eu(tta)_3(H_2O)_2]$ complex (Fig. S4†), the experimental intensity parameters Ω_λ (λ = 2 and 4), radiative (A_{rad}) and non-radiative (A_{nrad}) rates, lifetime (τ) values and emission quantum efficiencies (η) of the $^5D_0$ emitting level of the Eu^{3+} ion for the PMMA doped with $[Eu(tta)_3(H_2O)_2]$ were determined as described by Sá *et al.*[8] from the coefficients of spontaneous emission, according to the following expression:

$$\Omega_\lambda = \frac{3\hbar c^3 A_{0\lambda}}{4e^2\omega^3\chi\left\langle {}^7F_\lambda \| U^{(\lambda)} \| {}^5D_0 \right\rangle^2} \quad (1)$$

where χ is the Lorentz local field correction term, given by:

$$\chi = \frac{n(n^2+2)^2}{9} \quad (2)$$

and $\langle {}^7F_\lambda \| U^{(\lambda)} \| {}^5D_0 \rangle^2$ is a squared reduced matrix element whose value is 0.0032 for the $^5D_0 \rightarrow {}^7F_2$ transition and 0.0023 for the

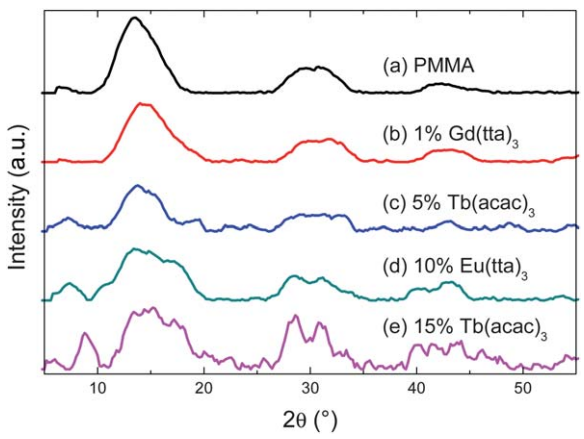

Fig. 1 Powder X-ray diffractions (XRD) of: (a) PMMA, (b) PMMA:1%$Gd(tta)_3$, (c) PMMA:5%$Tb(acac)_3$, (d) PMMA:10%$Eu(tta)_3$ and (e) PMMA:15%$Tb(acac)_3$.

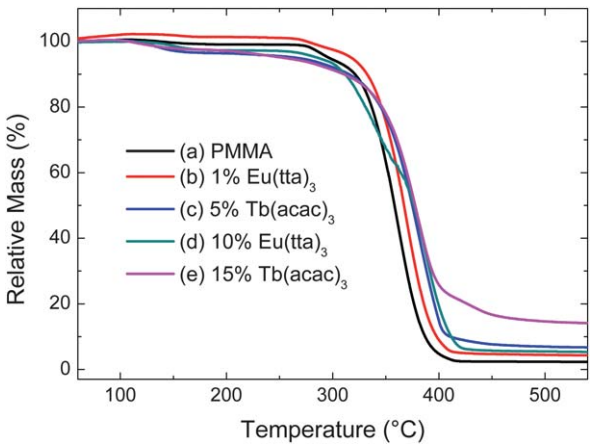

Fig. 2 Thermogravimetry analysis (TGA) curves registered under dynamic N_2 atmosphere of: (a) PMMA, (b) PMMA:1%$Eu(tta)_3$, (c) PMMA:5%$Tb(acac)_3$, (d) PMMA:10%$Eu(tta)_3$ and (e) PMMA:15% $Tb(acac)_3$.

$^5D_0 \rightarrow {}^7F_4$ one. The index of refraction n has been assumed equal to 1.5.[13]

In eqn (1) the $A_{0\lambda}$ ($\lambda = 2$ and 4) are spontaneous emission coefficients, calculated by taking the magnetic dipole transition $^5D_0 \rightarrow {}^7F_1$ as the reference, once this transition is practically insensitive to the chemical environment around the europium ion. The following expression was used:

$$A_{0\lambda} = A_{01}\left(\frac{S_{0\lambda}}{S_{01}}\right)\left(\frac{\nu_{01}}{\nu_{0\lambda}}\right) \quad (3)$$

where S_{01} and $S_{0\lambda}$ are the areas under the curves of the $^5D_0 \rightarrow {}^7F_1$ and $^5D_0 \rightarrow {}^7F_\lambda$ transitions, with ν_{01} and $\nu_{0\lambda}$ being their energy barycentres, respectively. The coefficient of spontaneous emission, A_{01}, in eqn (3) is given by the relation $A_{01} = 0.31 \times 10^{-11}(n)^3(\nu_{01})^3$, leading to an estimated value of around 50 s^{-1}.[8]

It is possible to determine the emission quantum efficiency (η) of the $^5D_0$ emitting level of the Eu^{3+} ion, according to eqn (4):

$$\eta = \frac{A_{rad}}{A_{rad} + A_{nrad}} \quad (4)$$

where the total decay rate is determined by:

$$A_{tot} = \frac{1}{\tau} = A_{rad} + A_{nrad} \quad (5)$$

where A_{rad} and A_{nrad} are the radiative and non-radiative rates, respectively, and A_{rad} is given by the expression:

$$A_{rad} = \sum_J A_{0\rightarrow J} \quad (6)$$

Thus, based on the experimental lifetime of the $^5D_0$ emitting level (τ) and A_{rad} rate, it was possible to determine the non-radiative rates (A_{nrad}).

Large Ω_2 values are attributed to the hypersensitive character of the $^5D_0 \rightarrow {}^7F_2$ transition of the Eu^{3+} ion, suggesting that the chemical environment around Eu^{3+} ion is highly polarisable in the present case and the dynamic coupling mechanism is quite operative (Table 1).[13,14] In addition, all the η values are higher than those for the Eu^{3+}-complex, indicating that the carbonyl groups of the polymeric matrix substitute water molecules in the first coordination sphere. Therefore, non-radiative decays induced by the vibrational modes of water molecule are decreased, providing an additional luminescence sensitisation channel in the energy transfer process from the organic moiety to the Eu^{3+} ion.[15]

Fig. 3(1) shows the excitation spectra of the PMMA:2%Eu-(tta)$_3$:15%Tb(acac)$_3$ (denoted as PE2T15) film with emission monitored at the $^5D_4 \rightarrow {}^7F_5$ (546 nm) (Fig 3(1a)) and $^5D_0 \rightarrow {}^7F_2$ (614 nm) (Fig 3(1b)) transitions of the Tb^{3+} and Eu^{3+} ions, respectively. It is observed three distinct absorption bands centred at 315, 330 and 380 nm which are assigned to the PMMA, acac and tta species, respectively. The overlap of these broad-band absorptions in the range from 240 to 400 nm enabled the selective sensitisation of the Eu^{3+} and Tb^{3+} ions.

It is observed that in the emission spectrum of the PE2T15 film (Fig. 3(2a)), under excitation at 380 nm (UVA), the $^5D_0 \rightarrow {}^7F_2$ transition (612 nm) originated from the Eu^{3+} ion is the most prominent in the visible range and is responsible for the subsequent red emission of the polymer film. On the other hand, under excitation from 240 to 315 nm (UVC and UVB), green emission is observed owing to the higher luminescence intensity of the $^5D_4 \rightarrow {}^7F_5$ transition (~545 nm) of the Tb^{3+} ion (Fig. 3(2c)). In addition, when the excitations are in the range from 315 to 380 nm the emission spectra of the film exhibit a combination of these two primary colours. For instance, the PE2T15 film produces yellow emission colour with excitation at 330 nm (Fig. 3(2b)). Therefore, this polymer film exhibits different emission colours under different excitation energy. The emission spectra of the Ln^{3+}–β-diketonate complexes doped in the PMMA matrix with [Eu]:[Tb] concentration ratios of 2 : 5, 2 : 10, 2 : 15 and 1 : 15 are shown in Fig. 3(3). Under excitation at 320 nm, the emission intensities of the $^5D_4 \rightarrow {}^7F_J$ transitions ($J = 0$–6) of the Tb^{3+} ion are progressively enhanced with the decrease of the [Eu]:[Tb] from 2 : 5 to 1 : 15. Consequently, the colour emitted by these films shifts gradually from red to green, yielding a luminescence tuning property by adjusting the doping concentrations of the two distinct Ln^{3+} emitting centres. Interestingly, the spectroscopic behaviour of these films depends indeed on the absolute concentration of each dopant rather than on the relative dopant proportion. This effect will be discussed in more detail later in this work.

Upon selective excitations and by varying the doping concentrations, the tuning of the luminescence is then achieved. This is illustrated by the CIE (*Commission Internationale de l'Éclairage*) x,y chromaticity diagram displayed in Fig. 4.[16] When the concentration ratio of the Eu^{3+}-complex *versus* the Tb^{3+}-complex increases, a gradual shift in the x,y colour coordinates from the green to the red spectral region is observed. On the other hand, the emission coordinates readily dislocate across the red–yellow–green region merely by increasing the excitation energy.

In order to understand the present phenomenon of colour tuneability, an intermolecular energy transfer (denoted as inter-ET) mechanism is evoked and evaluated using lifetime measurements for the PMMA films with different Ln^{3+}-complexes doping concentrations. Fig. 5(1) shows the normalised photoluminescence decay curves under excitation at 355 nm

Table 1 Experimental intensity parameters ($\Omega_{2,4}$), radiative (A_{rad}) and non-radiative (A_{nrad}) rates, lifetimes of the $^5D_0$ emitting level (τ) and quantum efficiencies (η) for the PMMA:x%Eu(tta)$_3$ systems

Samples	$\Omega_2/10^{-20}$ cm^2	$\Omega_4/10^{-20}$ cm^2	A_{rad}/s^{-1}	A_{nrad}/s^{-1}	τ/ms	η (%)
$[Eu(tta)_3(H_2O)_2]$[13]	33.0	4.6	923	2923	0.26	29
1%	43.0	10.4	1482	1788	0.31	45
5%	43.6	10.3	1497	1667	0.32	47
10%	43.6	10.5	1500	1554	0.33	49
15%	44.0	10.5	1513	1629	0.32	48

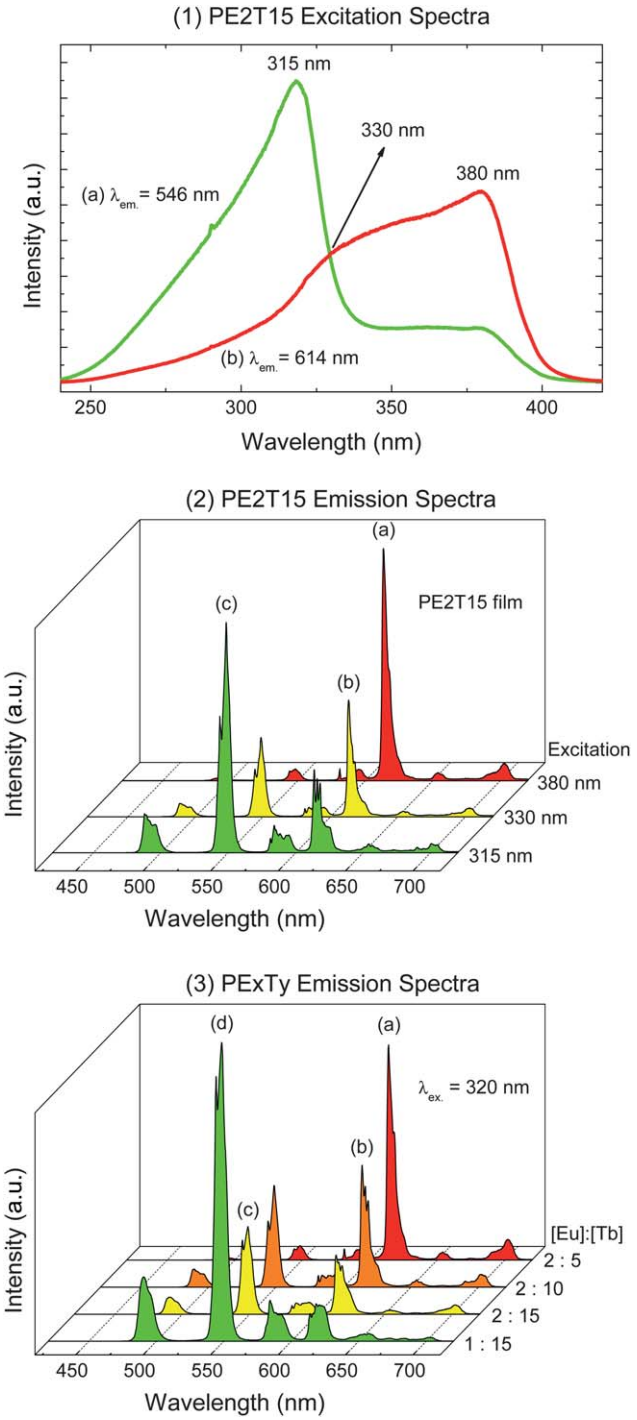

Fig. 3 (1) Excitation spectra with monitored emission at: (a) 546 nm and (b) 614 nm. (2) Emission spectra with excitation at: (a) 380 nm, (b) 330 nm and (c) 315 nm for PE2T15 film. (3) Emission spectra of PET films under excitation at 320 nm, where the [Eu]:[Tb] concentration ratios are: (a) [2 : 5], (b) [2 : 10], (c) [2 : 15] and (d) [1 : 15].

and monitored emission at 545 nm for PMMA:15%Tb(acac)$_3$ co-doped with x%Eu(tta)$_3$.

The inset in Fig. 5(1) shows the effect of the Eu^{3+}-complex concentration on the effective energy transfer rate (W_{ET}), determined by the equation:

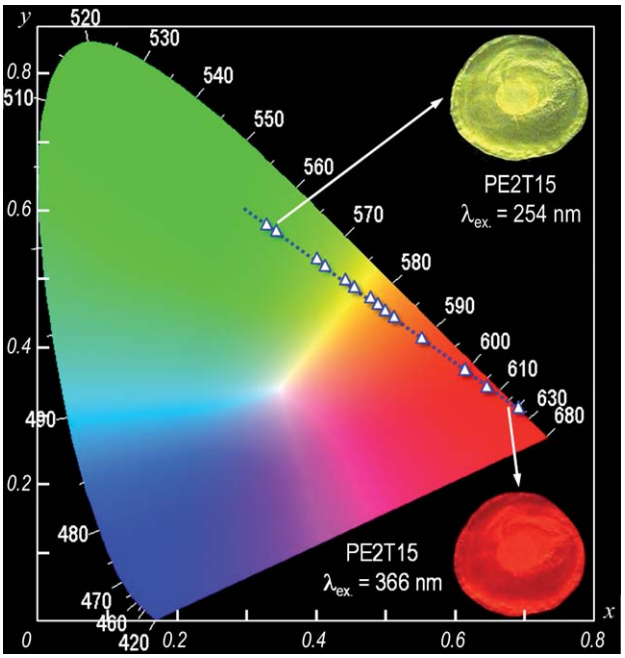

Fig. 4 CIE chromaticity diagram showing the x,y emission color coordinates for PMMA:Eu(tta)$_3$:Tb(acac)$_3$ films irradiated at different wavelengths. The inset figures are photographs of PE2T15 film taken with a digital camera displaying the green and red emissions under UV irradiation at 254 and 366 nm, respectively.

$$W_{ET} = \frac{1}{\tau_{Tb:Ln}} - \frac{1}{\tau_{Tb}} \quad (7)$$

where $\tau_{Tb:Ln}$ and τ_{Tb} are the lifetimes of the $^5D_4$ level in the presence and absence of other trivalent lanthanide ions (Ln^{3+} = Gd^{3+} and Eu^{3+}), respectively. The ultrafast energy injection of 5 nanoseconds at 355 nm prevents the polymer material from decomposition and selectively populates only the Tb^{3+} ions without activating the PMMA matrix or the Eu^{3+} ions. A trend of decreasing lifetime values (τ) of the $^5D_4$ emitting level of Tb^{3+} ions is observed (Table 2) with the increase of Eu^{3+}-complex concentration from 0 to 5%. Meanwhile, the W_{ET} also increases to 2.36×10^4 s^{-1}. This result indicates the existence of an energy transfer pathway which would deactivate the $^5D_4$ excited state of the terbium ion.

Further investigation was carried out by co-doping the [Gd(tta)$_3$(H$_2$O)$_2$] complex into the PMMA:Tb(acac)$_3$ films. It is noteworthy to mention that the first excited level ($^6P_{7/2}$) of the trivalent gadolinium ion is located at 32 000 cm^{-1}, which is far above the T_1 state of the β-diketonate ligands.[17] As a result, the emission spectrum of the Gd^{3+}-complex displays only the phosphorescence from the T_1 state, providing information on the structure of the energy levels of the ligand.[8,13]

Fig. 5(2) presents the normalised luminescence decay curves of PMMA:15%Tb(acac)$_3$ doped with Gd(tta)$_3$ with excitation at 355 nm and monitored emission at 545 nm, where the inset in Fig. 5(2) shows the effect of the Gd^{3+}-complex concentration on the W_{ET} transfer rate. It is noted a decrease in the lifetime values of the $^5D_4$ emitting level (τ) of the Tb^{3+} ions with the increase in Gd^{3+}–tta complex concentration (Table 2). The W_{ET} rate also increases till 3×10^4 s^{-1} as the Gd^{3+} complex concentration

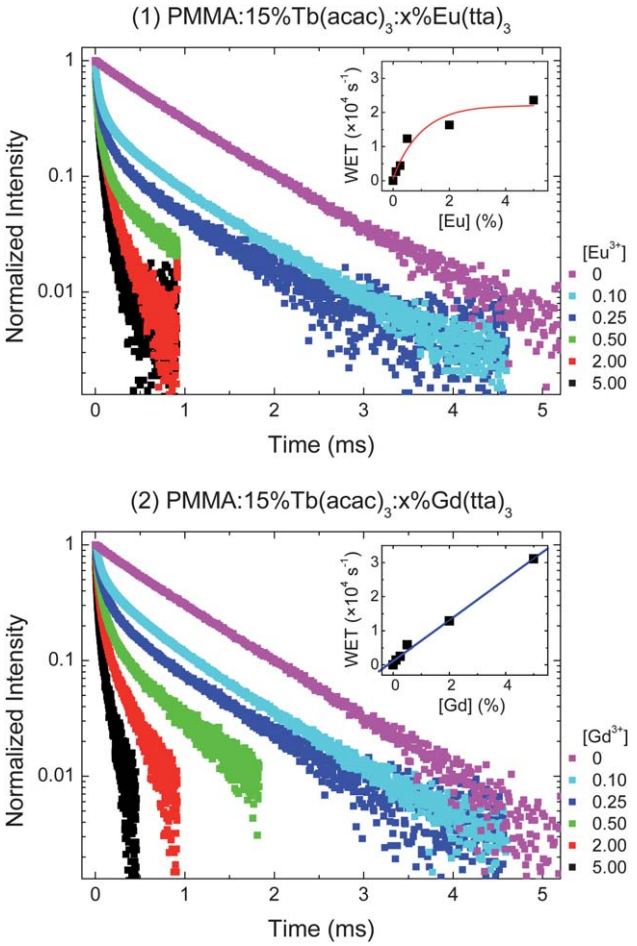

Fig. 5 Luminescence decay curves monitoring the excitation at 355 nm and emission at 545 nm of PMMA:15%Tb(acac)$_3$ co-doped with: (1) Eu(tta)$_3$ and (2) Gd(tta)$_3$. The inset figures show the curve of W_{ET} *versus* Ln^{3+} concentrations (Ln = Eu and Gd).

increases from 0 to 5%. This result indicates that the energy transfer occurs from the $^5D_4$ emitting level of Tb^{3+} ion to the T_1 state of the tta ligand. Therefore, the mechanism of inter-ET presented in Fig. 6 is evoked on the basis of the data leading to our interpretation on the $^5D_4$ lifetime decrease of the Tb^{3+} ion.

Moreover, in comparison with the Eu^{3+} doped systems, the doping with the Gd^{3+}-complex induces a significant increase of W_{ET} (Table 2). This can be assigned to the paramagnetic heavy ion effect that mixes the different multiplicities in the ligand,

Table 2 Lifetime values (τ) of the $^5D_4$ emitting level of the PMMA:15%Tb(acac)$_3$:*x*%Ln(tta)$_3$ where Ln = Eu and Gd, and the energy transfer rates (W_{ET})

	Eu^{3+}		Gd^{3+}	
$[Ln^{3+}]$ (%)	τ ($^5D_4$)/ms	$W_{ET}/10^4$ s^{-1}	τ ($^5D_4$)/ms	$W_{ET}/10^4$ s^{-1}
0	0.842	0	0.842	0
0.10	0.261	0.26	0.389	0.14
0.25	0.178	0.44	0.273	0.25
0.50	0.074	1.23	0.142	0.59
2.00	0.057	1.64	0.071	1.29
5.00	0.040	2.36	0.031	3.11

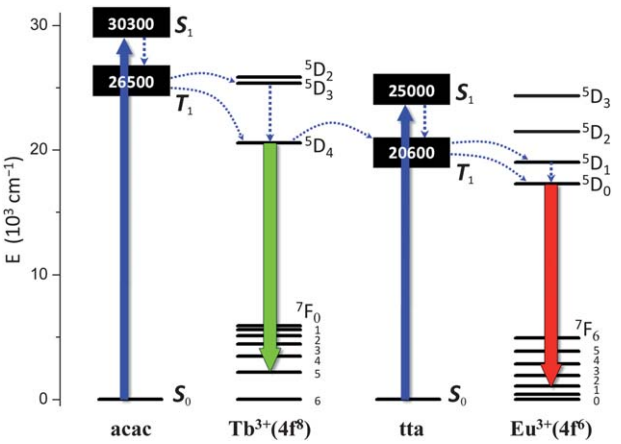

Fig. 6 Partial energy level diagram of the PMMA:Eu(tta)$_3$:Tb(acac)$_3$ polymeric system. The dashed arrows represent non-radiative decays and the most probable inter- and intramolecular energy transfer processes.

relaxing the spin selection rule.[2] This inter-ET mechanism also corroborates with the occurrence of different spectroscopic behaviours for the samples with equivalent concentration proportions. The final emitting colour is a combined result of the two lanthanide luminescent species and the inter-ET which depends on the distance between the two β-diketonate complexes dispersed in the PMMA matrix.

2.3. Photostability

The photostability of the Ln^{3+}-complexes and the doped polymer films was evaluated by monitoring the emission spectra intermittently under continuous exposure to UV irradiation for 6 hours using a 450 W xenon lamp as excitation source (Fig. 7).

Under UVA exposure at 330 nm, the luminescence intensities of the intraconfigurational $^5D_0 \rightarrow {}^7F_{0-4}$ (Eu^{3+}) (Fig. 7(1a)) and $^5D_4 \rightarrow {}^7F_{6-0}$ (Tb^{3+}) (Fig. 7(2a)) transitions suffer insignificant changes for the doped systems. However, the emission intensities decrease considerably for both the Eu^{3+} and Tb^{3+} ions when the film is exposed to UVC at 254 nm (Fig. 7(1b and 2b)), indicating the degradation of the luminescent species under higher energy irradiation. Overall, the doped polymer materials are more stable under UV irradiation than the individual complexes (Fig. 7(1c and 2c)). It is worth mentioning that the Eu^{3+} luminescence is slightly intensified upon UV irradiation (Fig. 7(1a)). This is probably due to the modification of the polymer surface and elimination of the defect within the texture/matrix after the UV light exposure,[18] whereas for the Tb^{3+} ion, the photodecomposition is the predominant process (Fig. 7(2)).

3. Experimental

Synthesis of [Ln(tta)$_3$(H$_2$O)$_2$] complexes

In 30 mL ethanol solution of 2-thenoyl-trifluoroacetone (1.0 g, 4.5 mmol), pH was adjusted to 6 using NaOH aqueous solution (0.01 mol L^{-1}). Subsequently, 20 mL aqueous solution of the hydrated lanthanide chloride ($LnCl_3 \cdot nH_2O$, 1.5 mmol) was added dropwise followed by the addition of 200 mL water. The formed precipitate was filtered, washed with pentane (10 mL)

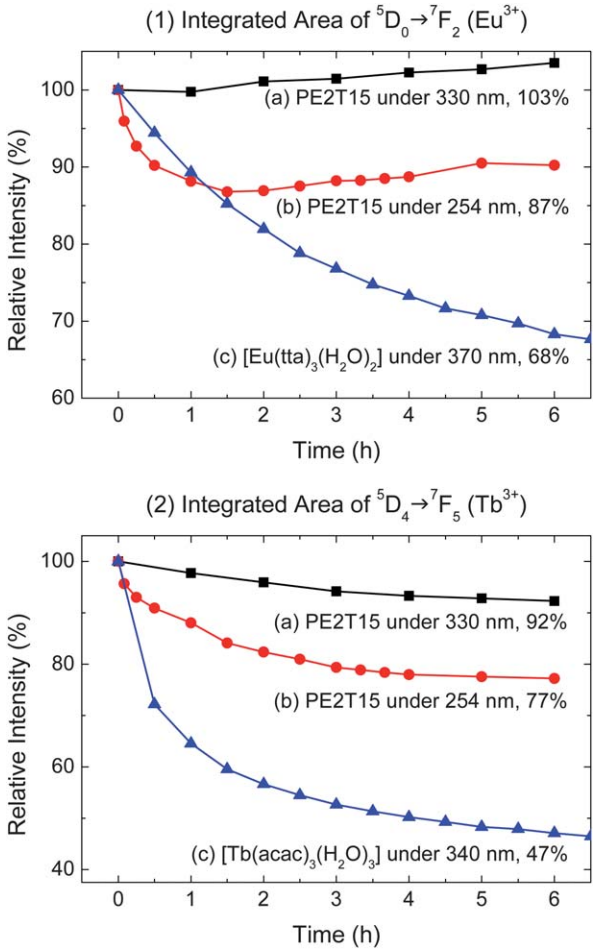

Fig. 7 Photostability comparison of the individual Ln^{3+}–β-diketonate complexes and PE2T15 film by monitoring the peak intensity of: (1) integrated area of $^5D_0 \rightarrow {}^7F_2$ transition (Eu^{3+}) and (2) integrated area of $^5D_4 \rightarrow {}^7F_5$ transition (Tb^{3+}).

and dried in vacuum (70%). (For $[Eu(tta)_3(H_2O)_2]$, found: C, 33.93; H, 1.92; Eu, 17.49. $C_{24}H_{16}F_9O_8S_3Eu$ requires C, 33.85; H, 1.89; Eu, 17.85%. For $[Gd(tta)_3(H_2O)_2]$, found: C, 33.79; H, 1.97; Gd, 18.24. $C_{24}H_{16}F_9O_8S_3Gd$ requires C, 33.64; H, 1.88; Gd, 18.35%.)

Synthesis of $[Tb(acac)_3(H_2O)_3]$ complex

Acetylacetone (0.60 g; 6 mmol) was dissolved in 30 mL of ethanol. NaOH (1 N; 6 mL) and a solution of hydrated lanthanide chloride ($TbCl_3 \cdot 6H_2O$, 0.56g; 1.5 mmol) in 10 mL of water were successively added to the solution of acac ligand. Water (100 mL) was added and the mixture was stirred for 2 hours. The precipitated complexes were filtered and then washed with water and dried in vacuum (85%). (Found: C, 34.94; H, 5.13; Tb, 31.55. $C_{15}H_{27}O_9Tb$ requires C, 35.31; H, 5.33; Tb, 31.14%.)

Preparation of PMMA film doped with Ln^{3+}-complexes

The PMMA powder (0.3 g) was dissolved in acetone (50 mL) followed by the addition of the required amount (from 1 to 15% in mass) of the Ln^{3+}-complexes in acetone solution. The mixed solution was heated at 60 °C for 30 minutes then cast onto a Petri dish. The polymer film was obtained after the total evaporation of the solvent at 60 °C.

Characterisation techniques

Carbon and hydrogen contents were determined by usual microanalytical procedures using an elemental analyser model CHN 2400 (Perkin-Elmer). Thermogravimetric analysis (TGA) was carried out with a TG/SDTA 822 thermobalance (Mettler-Toledo), using platinum crucibles containing at around 10 mg of the sample, under dynamic nitrogen atmosphere with a flux of 50 mL min^{-1}, at a heating rate of 5 °C min^{-1}. The infrared absorption spectra of the samples were measured by using a Bomem model MB102 FTIR spectrophotometer in the range of 4000–400 cm^{-1}. XRD patterns of the powders were recorded on a Rigaku Miniflex diffractometer using Cu K_α radiation (30 kV and 15 mA) from 2 to 90° (2θ) and 1 s of pass time.

Photoluminescence measurements

The excitation and emission spectra of the powdered and film samples were recorded in a SPEX Fluorolog-2 spectrofluorometer, model FL212 system, 450 W xenon lamp as excitation source and double grating 0.22 m SPEX 1680 monochromators. All spectra were recorded using a detector mode correction. The luminescence decay curves of the emitting levels were measured using a phosphorimeter SPEX 1934D accessory coupled to the spectrofluorometer. All spectral data presented in this work were recorded at room temperature (~298 K). The luminescence instruments were fully controlled by a DM3000F spectroscopic computer program and the spectral intensities were automatically corrected for the photomultiplier response. Excited states lifetime measurements were made using a third harmonic of a Continuum Q-Switch Nd:YAG laser (10 ns). The signals were recorded by an R928 photomultiplier coupled to a Tektronix TDS380 digital oscilloscope.

4. Conclusion

In summary, transparent substrate-free PMMA thin films with tuneable luminescence were prepared by a simple method under mild conditions. The β-diketonate complexes of trivalent europium and terbium were immobilised *via* chemical and physical interactions within the PMMA polymer matrix which also acts as co-sensitizer and enhances the luminescence. The emission properties of these multicolour films can be fine-tuned by both the adjustment of composition and excitation wavelength, exhibiting two individual primary colours, green and red, as well as the intermediate emission colours. The photoluminescence data suggest an intermolecular energy transfer from the $^5D_4$ level of the Tb^{3+} ion to the T_1 state of the tta ligands. To the best of our knowledge, it is the first time that such phenomenon is observed in polymer-based luminescent materials. Furthermore, the overall photostability of the luminescent species anchored in the polymeric matrix increased considerably in comparison to the individual Ln^{3+}–β-diketonates.

Acknowledgements

This work was supported by CAPES, CNPq, FAPESP, inct-INAMI, RENAMI and REDE-NANOBIOTEC-BRASIL (Brazilian agencies).

References

1 L. D. Carlos, R. A. S. Ferreira, V. de Zea Bermudez and S. J. L. Ribeiro, *Adv. Mater.*, 2009, **21**, 509; K. Binnemans, *Chem. Rev.*, 2009, **109**, 4283; S. V. Eliseeva and J.-C. G. Bünzli, *Chem. Soc. Rev.*, 2010, **39**, 189.
2 H. F. Brito, O. L. Malta, M. C. F. C. Felinto and E. E. S. Teotonio, in *Patai Series: The Chemistry of Metal Enolates*, ed. J. Zabicky, John Wiley & Sons Ltd., Chichester, England, 2009, ch. 3, pp. 131–184.
3 J. Kido and Y. Okamoto, *Chem. Rev.*, 2002, **102**, 2357; T. Oyamada, Y. Kawamura, T. Koyama, H. Sasabe and C. Adachi, *Adv. Mater.*, 2004, **16**, 1082; R. C. Evans, P. Douglas and C. J. Winscom, *Coord. Chem. Rev.*, 2006, **250**, 2093.
4 J. M. Bryson, K. M. Fichter, W.-J. Chu, J.-H. Lee, J. Li, L. A. Madsen, P. M. McLendon and T. M. Reineke, *Proc. Natl. Acad. Sci. U. S. A.*, 2009, **106**, 16913; H. Härmä, G. Sarrail, J. Kirjavainen, E. Martikkala, I. Hemmilä and P. Hänninen, *Anal. Chem.*, 2010, **82**, 892; H. Jiang, G. Wang, W. Zhang, X. Liu, Z. Ye, D. Jin, J. Yuan and Z. Liu, *J. Fluoresc.*, 2010, **20**, 321; J.-C. G. Bunzli, *Chem. Rev.*, 2010, **110**, 2729.
5 H. A. Höppe, *Angew. Chem., Int. Ed.*, 2009, **48**, 3572; G. He, D. Guo, C. He, X. Zhang, X. Zhao and C. Duan, *Angew. Chem., Int. Ed.*, 2009, **48**, 6132; K. T. Kamtekar, A. P. Monkman and M. R. Bryce, *Adv. Mater.*, 2010, **22**, 572.
6 R. C. Evans, L. D. Carlos, P. Douglas and J. Rocha, *J. Mater. Chem.*, 2008, **18**, 1100; B. K. Gupta, D. Haranath, S. Saini, V. N. Singh and V. Shanker, *Nanotechnology*, 2010, **21**, 055607.
7 L. Armelao, G. Bottaro, S. Quici, M. Cavazzini, M. C. Raffo, F. Barigelletti and G. Accorsi, *Chem. Commun.*, 2007, 2911; J. Yang, G. Li, C. Peng, C. Li, C. Zhang, Y. Fan, Z. Xu, Z. Cheng and J. Lin, *J. Solid State Chem.*, 2010, **183**, 451; C. M. Granadeiro, R. A. S. Ferreira, P. C. R. Soares-Santos, L. D. Carlos, T. Trindade and H. I. S. Nogueira, *J. Mater. Chem.*, 2010, **20**, 3313.
8 G. F. Sá, O. L. Malta, C. D. Donegá, A. M. Simas, R. L. Longo, P. A. Santa-Cruz and E. F. SilvaJr, *Coord. Chem. Rev.*, 2000, **196**, 165.
9 P. Leanaerts, K. Driensen, R. V. Deun and K. Binnermans, *Chem. Mater.*, 2005, **17**, 2148; B. Yan and H. Lu, *Inorg. Chem.*, 2008, **47**, 5601; S. Biju, M. L. P. Reddy, A. H. Cowley and K. V. Vasudevan, *J. Mater. Chem.*, 2009, **19**, 5179; P. P. Lima, F. A. A. Paz, R. A. S. Ferreira, V. de Zea Bermudez and L. D. Carlos, *Chem. Mater.*, 2009, **21**, 5099; P. Horcajada, T. Chalati, C. Serre1, B. Gillet, C. Sebrie, T. Baati, J. F. Eubank, D. Heurtaux, P. Clayette, C. Kreuz, J.-S. Chang, Y. K. Hwang, V. Marsaud, P.-N. Bories, L. Cynober, S. Gil, G. Férey, P. Couvreur and R. Gref, *Nat. Mater.*, 2010, **9**, 172; H. Peng, M. I. J. Stich, J. Yu, L. Sun, L. H. Fischer and O. S. Wolfbeis, *Adv. Mater.*, 2010, **22**, 716.
10 S. L. Hsu, in *Polymer Data Handbook*, ed. J. E. Mark, Oxford University Press Inc., New York, U.S.A. 1999, pp. 655–657; K. Lunstroot, K. Driesen, P. Nockemann, L. Viau, P. H. Mutin, A. Vioux and K. Binnemans, *Phys. Chem. Chem. Phys.*, 2010, **12**, 1879; W.-Q. Fan, J. Feng, S.-Y. Song, Y.-Q. Lei, G.-L. Zheng and H.-J. Zhang, *Chem.–Eur. J.*, 2010, **16**, 1903.
11 F. S. Richardson, *Chem. Rev.*, 1982, **82**, 541; F. J. Steemers, W. Verboom, D. N. Reinhoudt, E. B. van der Tol and J. W. Verhoeven, *J. Am. Chem. Soc.*, 1995, **117**, 9408.
12 D. F. Parra, H. F. Brito, J. R. Matos and L. D. Carlos, *J. Appl. Polym. Sci.*, 2002, **12**, 2716; B. Yan, *Mater. Lett.*, 2003, **57**, 2535.
13 O. L. Malta, H. F. Brito, J. F. S. Menezes, F. R. G. E. Silva, S. Alves, F. S. Farias and A. V. M. de Andrade, *J. Lumin.*, 1997, **75**, 255.
14 L. D. Carlos, Y. Messaddeq, H. F. Brito, R. A. S. Ferreira, V. de Zea Bermudez and S. J. L. Ribeiro, *Adv. Mater.*, 2000, **12**, 594.
15 M. D. McGehee, T. Bergstedt, C. Zhang, A. P. Saab, M. B. O'Regan, G. C. Bazan, V. I. Srdanov and A. J. Heeger, *Adv. Mater.*, 1999, **11**, 1349; J. Kai, D. F. Parra and H. F. Brito, *J. Mater. Chem.*, 2008, **18**, 4549.
16 P. A. Santa-Cruz, F. S. Teles, *SpectraLux Software v.1.0*, Ponto Quântico Nanodispositivos/RENAMI, 2003.
17 W. T. Carnall, G. L. Goodman, K. Rajnak and R. S. Rana, *J. Chem. Phys.*, 1989, **90**, 3443.
18 Q. Xu, L. Li, X. Liu and R. Xu, *Chem. Mater.*, 2002, **14**, 549; P. Nockemann, E. Beurer, K. Driesen, R. Van Deun, K. Van Hecke, L. Van Meervelt and K. Binnemans, *Chem. Commun.*, 2005, 4354; D. Wang, B. Li, L. Zhang, J. Ying and X. Wu, *J. Lumin.*, 2010, **130**, 598.

